A Graphical Approach to Automated Congestion Ranking for Signalized Intersections Using High-Resolution Traffic Signal Event Data

Peirong (Slade) Wang[1]; Swastik Khadka[2]; and Pengfei (Taylor) Li, Ph.D., P.E.[3]

Abstract: In recent years, high-resolution traffic signal event data has provided valuable insights into understanding and managing congestion at signalized intersections. While existing applications primarily employ automated traffic signal performance monitoring (ATSPM) systems as postanalysis tools for identifying everyday congestion causes, traffic engineers are increasingly overwhelmed by the number of ATSPM-capable intersections. The workload increases extensively as the number of ATSPM-capable intersections rises mainly due to the necessity of manually checking and generating performance figures. Nonetheless, an advanced ATSPM system capable of automatically detecting time-of-day congestion bottlenecks among multiple intersections and suggesting "top intersections of interest" would significantly aid traffic managers in monitoring historical congestion and preventing future congestion occurrences. This paper introduces an efficient graphical automated congestion ranking method for capable intersections, leveraging high-resolution traffic signal event data as the basis for automated congestion ranking. To accomplish these objectives, we build upon ATSPM concepts by continuously generating ATSPM measures of effectiveness (MOEs). Utilizing continuously generated ATSPM performance measures in Frisco, Texas, over several months, we devise an efficient graphical method for ranking hourly congestion levels among the studied ATSPM-capable intersections. All intersections are assessed and ranked using a multiobjective optimization technique, the Pareto front method. The points on the Pareto front represent dominating intersections with at least one inferior performance measurement, warranting prioritized improvement. The dominating points identified from the test dataset were validated and further explained using Purdue coordination diagrams (PCD), along with another individual dataset—Wejo-connected vehicle data. The outcomes of this approach have proven the validity of the method. **DOI: 10.1061/JTEPBS.TEENG-8083.**

Author keywords: Traffic signal systems; Automated traffic signal performance monitoring (ATSPM); Pareto front; Automated arterial management; Automated congestion ranking.

Introduction

Congestion is characterized by reduced travel speeds, extended vehicle queuing, and increased travel times. Over the past half-century, urban traffic congestion has grown significantly. According to INRIX Inc.'s 2021 congestion report (Pishue 2021), New York City ranked as the fifth most congested urban center globally and the first in the United States. Each driver in NYC lost 102 h in congestion. In Los Angeles, the I-5 South corridor from Euclid Ave to I-605 was the most congested in the United States, with peak hour delays of 22 min and accumulated to 89 h lost per driver in 2021. In 2019, the United States squandered 3.5 billion gallons of fuel and $190 billion, as reported by the Texas A&M Transportation Institute's 2021 Urban Mobility Report (David Schrank et al. 2021). Consequently, the U.S. Department of Transportation (USDOT) recognizes transportation system congestion as a significant threat to both the economic prosperity and the quality of life in the United States.

Intersections significantly contribute to congestion in urban areas, and congestion at intersections directly results from ever-increasing traffic demand. The most prevalent strategies to mitigate this issue include enhancing the intersection's capacity and improving traffic signal management; the key to increasing the capacity at intersections is controlling and managing conflicts between turning movements, and the newly proposed unconventional intersection design, exit lanes for left turns (EFL), is found to be effective in increasing intersection capacity, Zhao et al. (2019) proposed saturation rate adjustment models that resulted in a noteworthy 16% reduction in flow rate in demand starvation and lane changing scenarios, thereby substantiating the design's effectiveness. However, it is important to note that changing the physical geometry of existing intersections is not usually a feasible solution due to space constraints and infrastructure costs in built-up urban areas. Consequently, traffic signal management, which involves providing optimized signal timing plans, has become a more commonly adopted strategy to increase intersection capacity. Among various arterial traffic management efforts, the automated traffic signal performance monitoring (ATSPM) system has emerged as one of the most successful applications. The ATSPM system generates a series of novel signal performance measures of effectiveness (MOE) based on traffic signal events from traffic signal controllers. Consequently, an increasing number of agencies have adopted the ATSPM system.

[1]Graduate Research Assistant, Dept. of Civil Engineering, Univ. of Texas at Arlington, Arlington, TX 76019. ORCID: https://orcid.org/0000-0002-9636-7047. Email: peirong.wang@mavs.uta.edu

[2]Graduate Research Assistant, Dept. of Civil Engineering, Univ. of Texas at Arlington, Arlington, TX 76019. ORCID: https://orcid.org/0000-0002-5323-3081. Email: swastik.khadka@mavs.uta.edu

[3]Assistant Professor, Dept. of Civil Engineering, Univ. of Texas at Arlington, Arlington, TX 76019 (corresponding author). ORCID: https://orcid.org/0000-0002-3833-5354. Email: Taylor.Li@uta.edu

Note. This manuscript was submitted on May 9, 2023; approved on December 19, 2023; published online on February 28, 2024. Discussion period open until July 28, 2024; separate discussions must be submitted for individual papers. This paper is part of the ***Journal of Transportation Engineering, Part A: Systems***, © ASCE, ISSN 2473-2907.

Although the ATSPM system can provide insights into congestion causes, aggregating and visualizing the ATSPM MOEs is relatively slow. This limitation becomes more pronounced when examining MOEs for city-wide ATSPM-capable intersections, which can be excessively time-consuming for routine activities. This issue also hinders traffic managers from promptly identifying and mitigating unusual congestion.

The existing congestion measurement methods can be broadly categorized into mobility measures and reliability measures. Mobility measures encompass various indicators, such as travel delay, volume-to-capacity ratio (V/C ratio), level of service (Barcelö et al.), and the travel time index. The travel time index is defined as the average peak travel time ratio to the off-peak standard travel time. On the other hand, reliability measures include the buffer index, which represents the additional time required to ensure on-time arrival for most trips, and the planning time index, which is statistically defined as the 95th percentile of the travel time index. The planning time index reflects the extra time most travelers allocate when planning trips during peak periods. For example, a value of 1.60 indicates that travelers plan for an additional 60% travel time above the off-peak travel times to ensure a 95% on-time arrival rate. It is important to note that these methods are better suited for assessing congestion on freeways, where data records are often available in large volumes. However, applying these methods to measure congestion at intersections is challenging. Predominant methods, such as level of service, average delay, and queue length, require calibrated advanced detectors and stop bar detector locations to accurately capture vehicle arrival and departure profiles (Sharma et al. 2007). However, finding the optimal sensor placement is challenging, as it varies from site to site and several other parameters, like storage capacity per lane at the intersection, saturation headway, and queue clearance headway, must be measured. These parameters are not standard for ATSPM setup and require extensive manual collection, which can be burdensome when managing hundreds or even thousands of intersections.

The commercial market offers a range of software solutions for identifying coordination and signal timing issues in traffic management. Among these, Q-free's Kinetic Signals is built upon the MAXVIEW advanced traffic management system (Q-Free 2023). This system is designed to control and adjust traffic signals in conjunction with real-time intelligent transport system (ITS) operations. Kinetic Signals provides a real-time map for managing signalized intersections, offering detailed operational information, including device statuses and measurements. The platform also features a system for collecting and reporting high-resolution signal events that integrates ATSPM, graphical data, and usage charts for analysis. TranSync (TransIntelligence 2023), another solution in this field, focuses on the diagnosis and optimization of signal timing. It aims to systematically manage, optimize, and evaluate traffic signal timing plans. TranSync-M, its mobile version, comprises a virtual controller, dynamic time-space diagram, signal timing editor, and trajectory recorder. This enables real-world programmed signal timings to create detailed visualizations of signal coordination plans. Additionally, TranSync allows users to record their GPS location and trajectory data in real time, facilitating the combination of before-and-after video clips for comprehensive analysis. While both MAXTIME Kinetic Signals and TranSync are mature and powerful tools, they still fall short of automation. Given that cities or counties can manage hundreds of intersections, the efforts in manual visualization and analysis based on the ATSPM data can be excessively complicated and time-consuming. As a result, many agencies expressed a need for a more streamlined approach to exploiting the ATSPM's potential: one that incorporates a ranking method based on ATSPM data. This would allow engineers to automatically pinpoint intersections that warrant further investigation on a daily basis.

To address these challenges, an automated congestion ranking framework grounded in ATSPM concepts is developed to pinpoint time-of-day mobility bottlenecks on arterials. The ranking results offer decision support for traffic managers, allowing them to identify the latest bottlenecks among hundreds or even thousands of intersections and promptly provide solutions. The remainder of this paper is structured as follows: literature review, data preparation, methodology description, and case studies.

Literature Review

Traffic congestion, experienced by road users as stops or slow movements on freeways, suburban highways, or city streets, occurs when (1) the road system is unable to accommodate travel demand, and (2) traffic control at intersections is improperly configured. Traditional congestion measures include travel time, delay, and speed, while other measures such as travel rates, delay ratios, mobility index, congested travel, and accessibility also exist. Congestion can be described by four attributes: duration, extent, intensity, and reliability. Duration is defined as the amount of time congestion affects the mobility of the system; extent is described by the number of people or vehicles affected by congestion; intensity reflects the severity of the congestion that affects travel, it is used to differentiate between levels of congestion, and reliability is the impact of nonrecurrent congestion on the transportation system such as congestion caused by weather and accidents.

Traffic congestion at intersections can occur due to various reasons. One common cause is excessive demand beyond the intersection capacity. Another cause is due to inferior traffic signal systems, such as out-of-date timing plans and/or broken detectors. Another cause is the problematic intersection geometry designs that offer insufficient lanes to accommodate demand. Nonrecurring bottlenecks like obstructed or blocked lanes by accidents or work zones also contribute to congestion at intersections. Once a problematic intersection is identified, there are multiple practical approaches to improvement like optimizing traffic signal timings, implementing new ITS solutions, or redesigning the intersection layout. Nonetheless, it is challenging to identify those intersections in need of immediate congestion alleviation among hundreds or even thousands of candidates managed by agencies.

In practice, complaints from nearby residents have become a de facto benchmark to identify problematic intersections. There are plenty of broadly accepted performance data collecting methods, including but not limited to the Wi-Fi/Bluetooth MAC readers (Abbott-Jard et al. 2013; Barcelö et al. 2010), Sensys Networks reidentification sensors (Pitton et al. 2012), and personal probe device traffic data collection [e.g., INRIX (Pishue 2021)]. Nonetheless, these solutions are effective at the corridor level but may not be reliably effective at individual intersections. ATSPM is a state-of-the-art traffic signal monitoring concept. It refers to a collection of data analytics tools and approaches that automatically collect and convert high-resolution traffic controller event data into actionable performance measures. Most deployed ATSPM can continuously collect and generate high-resolution signal performance measures on capable approaches of intersections and is becoming a regular tool among agencies today.

The evolution of signal performance measures can be divided into two stages: In the first stage, performance measures primarily relied on manual data collection or semiautomation, requiring many time-consuming processes. Performance metrics varied among systems and were constrained in scope and granularity.

During this era, straightforward measures such as vehicle delays, queue lengths, and green time usage were the research focus. Balke and Herrick (2004) proposed using average cycle time, average phase duration, average wait time before serving a call, and the average proportion of green used to serve a queue to measure signal efficacy. Expanded from this research, Balke et al. (2005) further developed the Performance Measure Report Generator (PMRG) to automatically collect signal events and generate reports based on signal performance data.

In 2007, Smaglik et al. from Purdue University developed a data collection module for NEMA traffic controllers, enabling quantitative assessment of progression and intersection delay (Smaglik et al. 2007). This work was a milestone of the ATSPM development and formed the foundation of today's ATSPM systems. Subsequently, Day et al. presented performance measures for evaluating operations (Day et al. 2008), such as phase-based arrival versus green window, split failure plot, and time-of-day volume-to-capacity ratio plot. Liu and Ma developed *SMART-SIGNAL*, a system for real-time high-resolution traffic signal data collection and performance measure generation based on probe vehicle trajectories and signal data (Liu and Ma 2009). Brennan Jr.et al. further developed visualization techniques for intersection coordination, such as time-of-day schedule change time, cycle length, preemption, and queuing analysis (Brennan et al. 2011). Indiana Department of Transportation and Purdue University built upon Smaglik et al.'s work and published the Indiana Traffic Signal Hi-Resolution Data Logger standard (Sturdevant et al. 2012). Grossman et al. deployed the first commercial ATSPM solution in Indiana (Grossman and Bullock 2013). Day et al. discussed methodologies for data collection and introduced various performance measures (Day et al. 2014). Day et al. published a report that provided resources for agencies developing active traffic management programs (Day et al. 2016). Following the Traffic Signal Systems Operations & Management pool fund study in the same year, UDOT released its open-source ATSPM system (US DOT 2018), which is widely used today. Remias et al. implemented multiple ATSPM systems including UDOT's ATSPM software on 11 signals at US 36 (Pendleton Pike) in Indianapolis, Indiana, demonstrating the full capacity of using ATSPM systems with high-resolution signal event data performing capacity, signal progression, multimodal (pedestrian, preemption and priority), and maintenance performance measures. (Remias et al. 2018). Jin et al. enabled ATSPM measurements for nonhigh-resolution signal controllers and historical signal event records from InSync and SCATS systems (Jin et al. 2019). Li et al. proposed a framework combining real-time LOS and probe vehicle data with ATSPM systems (Li et al. 2020). The proposed framework introduces a novel diagram that incorporates ATSPM data from multiple intersections to enable corridor-level monitoring with two additional performance measures designed: arrival on coordination (AOC) and band attainability (BA) to measure the signal coordination quality.

Pareto Front: In the realm of resource allocation and economic efficiency, the concept of the Pareto front originates in the work of Italian economist Vilfredo Pareto, who initially introduced the idea of Pareto optimality. Over time, the Pareto front—also known as the Pareto frontier—has become an essential tool for multiobjective optimization and decision making. American mathematician and economist Kenneth Arrow and French economist Gérard Debreu made significant advancements in developing the Pareto front concept. In their seminal paper, Arrow and Debreu applied Pareto optimality to general equilibrium theory, proving the existence of Pareto optimal allocations in a competitive economy (Arrow and Debreu 1954). Ngatchou et al. discussed the fundamentals of multiobjective optimization and different solution approaches to generating the Pareto front (Ngatchou et al. 2005). In the context of multiobjective optimization, each potential solution is assessed according to its performance across multiple objectives. A solution is deemed Pareto optimal if no other solution can enhance one of the objectives without concurrently worsening at least one other objective. Put differently, a Pareto optimal solution cannot be outperformed (also known as dominated) by any other solution whose objective measures are all better than the Pareto optimum. In a graphical representation of a two-objective optimization problem, the Pareto front can be visualized as an envelope curve or a set of points in the objective space, where one axis represents one objective, and the other axis represents the other objective. Each point on the Pareto front represents a solution that is not dominated by any other solution in terms of the objectives being considered.

Pareto front analysis is widely utilized within the transportation research community. Abbas and Sharma employed a multiobjective nondominated sorting algorithm to determine the Pareto front across three objective optimizations: delay, stops, and degree of detachment (DoD) (Abbas and Sharma 2006). They subsequently created an optimal timing plan based on the Pareto front. Jiao et al. implemented a Pareto front-based multiobjective real-time traffic signal control model for intersections (Jiao et al. 2016). The results illustrated that their proposed method surpassed the performance of the existing multiobjective traffic control model that consolidates several objectives into a single target of weighted summation. Chellapilla et al. introduced innovative bilevel mathematical programming models and solved through Pareto front analysis, ensuring system optimality and minimizing congestion on overly utilized links while considering user needs as constraints (Chellapilla et al. 2023).

Methodology and ATSPM Data Aggregation

This paper aims to assist agencies in ranking intersection congestion utilizing historical MOE data, thereby identifying the most problematic intersections without the need to visualize the performance measures for each. The proposed methodology will enable agencies to swiftly identify spatial and temporal aspects of underperforming intersections or approaches. Traffic managers can utilize their ATSPM systems for in-depth analysis of these congested intersections, aiding in informed decision making. Fig. 1 illustrates the framework of the proposed method. The left section, Fig. 1(a), outlines the workflow, encompassing automated Steps 1 to 6. Step 7, highlighted with a dashed line, varies in automation depending on the ATSPM system in use. In the experiment of this paper, the UTA-in-motion ATSPM system facilitates fully automated plotting of coordinate diagrams (PCDs). In contrast, with the UDOT ATSPM system, this process would require manual intervention. Fig. 1(b) presents a logical chart from Steps 2 to 6, elucidating the method's decision process.

By default, the prevalent open-source and commercial ATSPM systems in the market save high-resolution signal control events (i.e., raw data) periodically. The ATSPM MOEs are not automatically generated but on users' requests. The ATSPM MOEs are the building blocks of the automated congestion ranking and generating them for all intersections will take a long time. Therefore, generating the ATSPM MOEs continuously rather than upon the user's request is critical to ensure the needed time for automated congestion ranking is acceptable. The details of the whole process are as follows:

- Step 1: Develop an add-on ATSPM module to automatically generate ATSPM MOEs on all possible approaches at a 5-min interval, the selected MOEs include arrival-on-green (AOG), AOC,

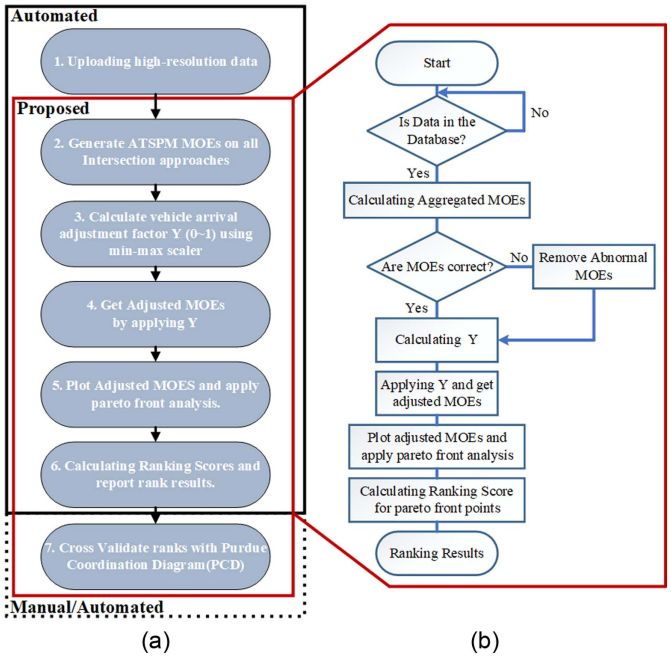

Fig. 1. Automated congestion ranking framework using ATSPM data: (a) flow chart; and (b) logical relationship.

green-time-percentage (GT), vehicle arrival counts (veh_arr), the number of pedestrian's crossing quests (ped_button), TOD plan transition (plan_change), and day of the week (DOW).

- Step 2, The generated 5-min MOEs can be further aggregated to various time intervals. In this paper, we transfer 5-min MOEs to 1-h MOEs.
- Step 3: This paper incorporates the min-max normalization technique to mitigate the issue of disadvantaged off-peak and low-performance side streets due to the low vehicle arrival rates in the Pareto front analysis. This approach transforms the vehicle arrival numbers into a standardized scale from 0 to 1. The minimum and maximum values used for this normalization are derived from historical arrival data encompassing the entire testing scope and are specific to the selected time range. These normalized values are then used as an adjustment factor in the subsequent analysis.
- Step 4: Aggregate the MOEs according to the DOW within the same month, the hour of day, and signal phases. For instance, the aggregated ATSPM MOEs from 7:00 AM to 8:00 AM on Mondays in November of 2021 were calculated as the average of the MOEs on five Mondays in that month. A vehicle adjustment factor Y will then be multiplied to such aggregated MOEs for further Pareto front analysis.
- Step 5: Pareto front analysis: three selected ATSPM MOEs are arrival-on-green (AOG), AOC, and GT. These MOEs are directly associated with signal timing and represent intersection congestion conditions. To obtain adjusted AOG, AOC, and GT, we multiply these MOEs by the normalization factor (Y) derived in Step 4. After conducting the Pareto front analysis, we obtain the data points on the Pareto front that represent the worst traffic conditions with respect to time periods, locations, and approaches.
- Step 6: Inform traffic managers to generate ATSPM diagrams to identify the congestion and its causes based on Pareto sets from the last step. Some mitigation measures will be taken to prevent similar congestion in the future if necessary.

ATSPM MOE Aggregation

Traffic signal events data are a set of time-stamped records containing number-encoded event types and event indexes. For example, the Indiana Traffic Signal Hi-Resolution Data Logger Enumeration guideline defines event number 7 as termination of a green phase and the following event index represents signal phase ID. The signal events' time stamps are in a 10 Hz frequency of 0.1 s. The original traffic signal events must be aggregated to MOEs to become actionable, such as arrival-on-green (AOG), AOC, and GT, arrival on red (AOR) and not-AOC (NAOC). The definitions of AOG, AOC, AOR, GT, and NAOC are as follows:

$$\text{AOG} = \frac{v_{gt}}{V_t} \tag{1}$$

$$\text{AOR} = 1 - \text{AOG} \tag{2}$$

$$\text{AOC} = \frac{v_{ct}}{V_t} \tag{3}$$

$$\text{NAOC} = 1 - \text{AOC} \tag{4}$$

$$GT = \frac{g_t}{t} \tag{5}$$

where v_{gt} = vehicle arrivals during green within time interval t; V_t = total vehicle arrival during time interval t; v_{ct} = vehicle arrivals within the coordinated green band during t; and g_t = accumulated green time during t.

In the automated MOE aggregation module, the default time interval is 5 min. It is configured this way for three reasons: first, the cycle lengths of coordinated traffic signal timing typically range between 60 and 180 s and 300 s ensure covering at least one complete cycle. Second, the signal events collected within 5 min can be processed quickly. Third, a 5-min time interval represents the shortest period of agencies' interest and the 5-min MOEs can be further aggregated to longer periods as per agencies' request as follows:

$$\text{MOE}_T = \frac{\sum_{t=1,2,..}^{T} \text{MOE}_t}{\sum T} \tag{6}$$

where T = number of 5-min intervals; MOE_T = aggregated MOE (AOG, AOR, AOC, NAOC, and GT) within $5 \times T$ min (e.g., $T = 2$ means a 10-min interval); MOE_t = MOE of the tth 5 min.

Pareto Front Construction

Pareto dominance is a method of multiobjective optimization to identify nondominated solutions that represent the most favorable trade-offs between multiple competing objectives. The Pareto front comprises the set of all nondominated solutions. A solution is on the Pareto front if there is no other solution that is better for all objectives. This approach is widely employed in engineering, planning, and decision making processes, where the objective is to discover the most balanced solutions among several objectives, which may be subject to either minimization or maximization. To determine the Pareto front for a two-objective problem, consider two solutions (X_1, Y_1) and (X_2, Y_2) in a maximization scenario. If $X_1 >= X_2$ and $Y_1 >= Y_2$, then (X_1, Y_1) "dominates" (X_2, Y_2) in terms of both objectives. Conversely, in a minimization problem, (X_2, Y_2) "dominate" (X_1, Y_1). The search iterates until no more dominating point can be found. Those dominating points are composed of the Pareto front.

J. Transp. Eng., Part A: Systems, 2024, 150(5): 04024017

Ranking Score Calculation

Ranking dominating points is performed by calculating the ranking score as in Eq. (7):

$$R_{\text{score}} = A_{\text{score}} + B_{\text{score}} \tag{7}$$

A_{score} and B_{score} = considered parameters in the Pareto front analysis. For example, if we wish to identify the Pareto front searching with respect to the arrival-on-red value or A_{score} and the red-time percentage value $(1 - GT)$, or B_{score} as a maximization problem. The data point with the highest R_{score} represents the most congested scenario in which most vehicles arrive on red and stop because the red time lasts long.

Scenario Design

Three scenarios are selected according to agencies' various needs: The first scenario is to examine the relationship between AOR and GT maximization to identify the occasions when an intersection reports most vehicles arrived during red despite of long allocated green time. Unbalanced green allocations will likely cause this phenomenon.

The second scenario aims to discover the Pareto front with respect to the vehicle arrivals on green but not the result of coordination (not-AOC) or NAOC and vehicle AOR. We seek to identify occasions when a poorly coordinated timing plan causes most upstream vehicles to arrive at the downstream intersection too early or too late.

The third scenario is to discover the Pareto front concerning NAOC and GT. The target occasions are when an intersection is allocated with excessively long green time while many vehicles arrive before or after the green band (i.e., they indeed arrive on green at the downstream intersection, but it is not due to effective signal coordination).

In all the presented three scenarios, the dominating occasions with the worst ranking score are identified in which heavy congestion occurred because of various traffic signal timing problems. Once the worst scenarios are identified, full-scale visualizations of ATSPM MOEs of the corresponding scenarios should be performed for agencies to find valid reasons for congestions.

Note that, other than the traffic signal problems, accommodations for special traffic signal operations like preemption or transit signal priority can also cause heavy delays. The signal timing problems can be easily observed from a fully populated visualization of ATSPM MOEs.

The algorithm for constructing the Pareto Front can be as follows:

Algorithm. Identify dominated solutions as maximize problem using Pareto front

Data: $\boldsymbol{X}$ the value set of target variable A; $\boldsymbol{Y}$ the value set of target variable B; $\boldsymbol{W}$ is a list of tuples where each tuple is represented by $(\boldsymbol{X_i}, \boldsymbol{Y_i})$; $\boldsymbol{Z}$ is a dominant list, contains identified Pareto front points.
Results: For finding Pareto in front of target variables A and B.
Initialize the empty list $\boldsymbol{Z}$ for dominant points,
Initialize the sorting list $\boldsymbol{W}$ in ascending order based on the value $(\boldsymbol{X'}, \boldsymbol{Y'})$.
For $\boldsymbol{X_i}$ in the range of all points of variable A:
Do Save the first point $\boldsymbol{X'}, \boldsymbol{Y'}$ to list $\boldsymbol{Z}$,
Set 'is dominant' flag to False,
For each point $(\boldsymbol{X'}, \boldsymbol{Y'})$ in list $\boldsymbol{W}$:
if $\boldsymbol{X' \leq X_i}$ and $\boldsymbol{Y' \leq Y_i}$:
Set 'is dominant' True.
Do save $(\boldsymbol{X'}, \boldsymbol{Y'})$ to dominant list $\boldsymbol{Z}$.
Break
If $\boldsymbol{X' \leq X_i}$ and $\boldsymbol{Y' \leq Y_i}$:
Set 'is dominant' False.
Do remove $(\boldsymbol{X_i}, \boldsymbol{Y_i})$ from list $\boldsymbol{W}$.
End
End

Case study: Using ATSPM to Identify Arterial Bottleneck Pattern and Causes on Preston Road in Frisco, Texas

Data Preparation

The authors retrieved two months of traffic signal logs from five intersections along Preston Road in Frisco, TX, from October to November 2021 and aggregated them into the proposed ATSPM MOEs on all available approaches every 5 min. In total, 351,600 5-min ATSPM MOEs were generated. After transforming to hourly MOEs, 5,655 hourly ATSPM MOE records were obtained. Fig. 2 shows the locations of the intersections. Intersections 670, 673, 675, and 680 are along the Preston Road, and Intersection 639 is next to a large high-rise shopping mall. Fig. 3(b) illustrates that traffic volumes passing through Intersections 680 and 639 are greater during weekends than on weekdays.

Based on the preliminary data analysis, ATSPM data for Phase 2 at Intersection 639 were preexcluded from the case study because

Fig. 2. Scope of study in Frisco, TX. (Google Map Data © 2023.)

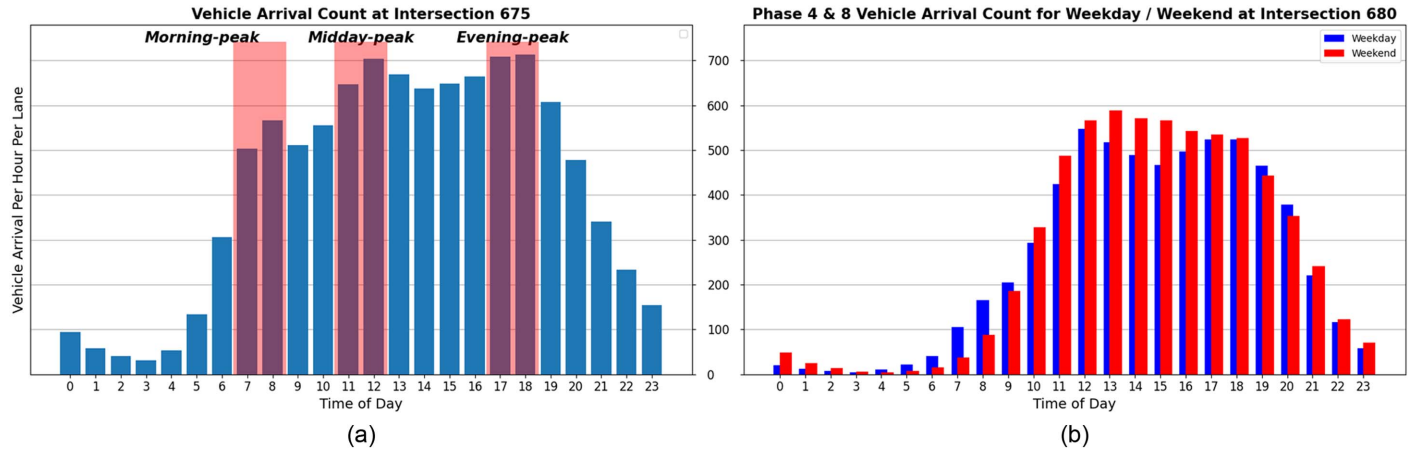

Fig. 3. Time-of-day traffic count plot: (a) weekday Preston Road volume at 675; and (b) weekday and weekend side street volume comparison at 680.

of its malfunctioning detectors during the study period. Phase 4 of Intersection 670 and Phase 4 at Intersection 673 were also excluded because the vehicle arrivals were unrealistically low, possibly caused by intermittent detector errors or network connection errors. It was also found that some AOC MOEs had zero values because of intermittent detector malfunctions at upstream and/or downstream intersections. Zero AOC values (i.e., seemingly rather poor signal coordination) may bring significant bias to the congestion scenario ranking. As such, whenever a zero AOC value is identified, the algorithm automatically excludes that scenario from being considered as dominating or a candidate for the worse scenario.

To analyze the traffic volume pattern on Preston Road, Intersection 675—the central intersection—was chosen for a time-of-day traffic counts analysis. Based on Fig. 3(a), three distinct peaks were identified. The morning peak runs from 7 AM to 8 AM, recording 565 vehicles per hour per lane. The midday peak is from 11 AM to 1 PM with a volume of 704 vehicles per hour per lane. Lastly, the evening peak starts at 5:00 PM and concludes at 6:00 PM, noting 713 vehicles per hour per lane. The traffic between the morning and evening peaks predominantly reflects regular commuters to work and school, while the midday peak is due to the commercial activities near that area, based on Fig. 3(b), the midday peak counts are observed much higher during the weekend than weekdays. These peak hours are utilized in Experiments II and III.

Experiment I: Identifying the Most Congested Hour of All Times among All Intersections

This experiment aims to better inform agencies when and where traffic is the most congested by identifying the most congested time of day, month, intersection, and phase. So, the agencies can allocate more resources for congestion reduction. We first analyzed the hourly aggregated MOEs on all approaches at all intersections to determine which intersection historically exhibited the poorest performance on average according to the ATSPM dataset. Each record is indexed with the hour of the day, the associated phase number, and the intersection ID. Each record was averaged with multiple weeks over 2 months of ATSPM data and MOEs.

Fig. 4 presents three 2-D Pareto fronts and a 3-D Pareto surface for the GT, AOR, and NAOC MOEs respectively. The red lines in Figs. 4(a–c) represent the Pareto fronts on which those dominating intersections (with at least one worst mobility performance) reside and the top-ranked Pareto front point is circled in red for each Pareto analysis. The black solid line in Figs. 4(a and c) delimit between actual positive AOC data, containing zero values, and the adjusted AOC values to address the missing data issue. As discussed, the adjusted NAOC values are therefore consistently negative to ensure those intersections with data missed could not become dominating (i.e., worst) intersections.

Table 1 displays the top three results from each Pareto front depicted in Fig. 4. To validate the ranking results, a complete ATSPM diagram (the "ground truth") is generated to confirm if the identified bottleneck exists. For the sake of brevity, the ATSPM plot for the highest-ranked Pareto point is included; this can be found in Fig. 5.

From the Pareto Frontier in Fig. 4, three time-dependent bottlenecks were selected for verification:

1. Phase 4 at Intersection 639 from 1:00 PM to 2:00 PM on Saturdays in November 2021 with low AOC rates.
2. Phase 2 at Intersection 670 from 8:00 AM to 9:00 AM on Tuesdays in November 2021, experiencing excessive AOR.
3. Phase 8 at Intersection 680 from 3:00 PM to 4:00 PM on Sundays in November 2021 has a high number of vehicles on red and not arriving on coordination.

The identified bottlenecks were verified with fully populated ATSPM MOE diagrams on selected dates. For the first identified bottleneck, Fig. 5(a) reveals two preemption calls from two directions, disrupting the coordination plan and leading to a decrease in vehicles arriving during coordination. This implies that frequent traffic signal operations may have caused the bottleneck; Fig. 5(b) indicates quite a few vehicles arriving during the red time, and a preemption call is observed on Phase 4 that interrupted the programmed coordination plan; Fig. 5(c) displays another dominating road approach at Intersection 680 that was identified in Fig. 4(c). The ATSPM plot reveals that most vehicles arriving during the red on that phase and two preemption events exacerbate the situation. This implies that Intersection 680 may need to be retimed with clock-based coordination.

Experiment II: Identifying the Dominating Roach Approaches Having Bottlenecks during Weekday Peak Hours

In this experiment, ATSPM records were chosen explicitly from Monday to Friday during the morning peak hours (8 AM–10 AM), midday peak hours (11 AM–1 PM), and evening peak hours (6 PM–8 PM). In Fig. 6, the line located in the top-right corner illustrates the Pareto fronts under three different conditions, along with the top-ranked points, which are denoted by circles positioned

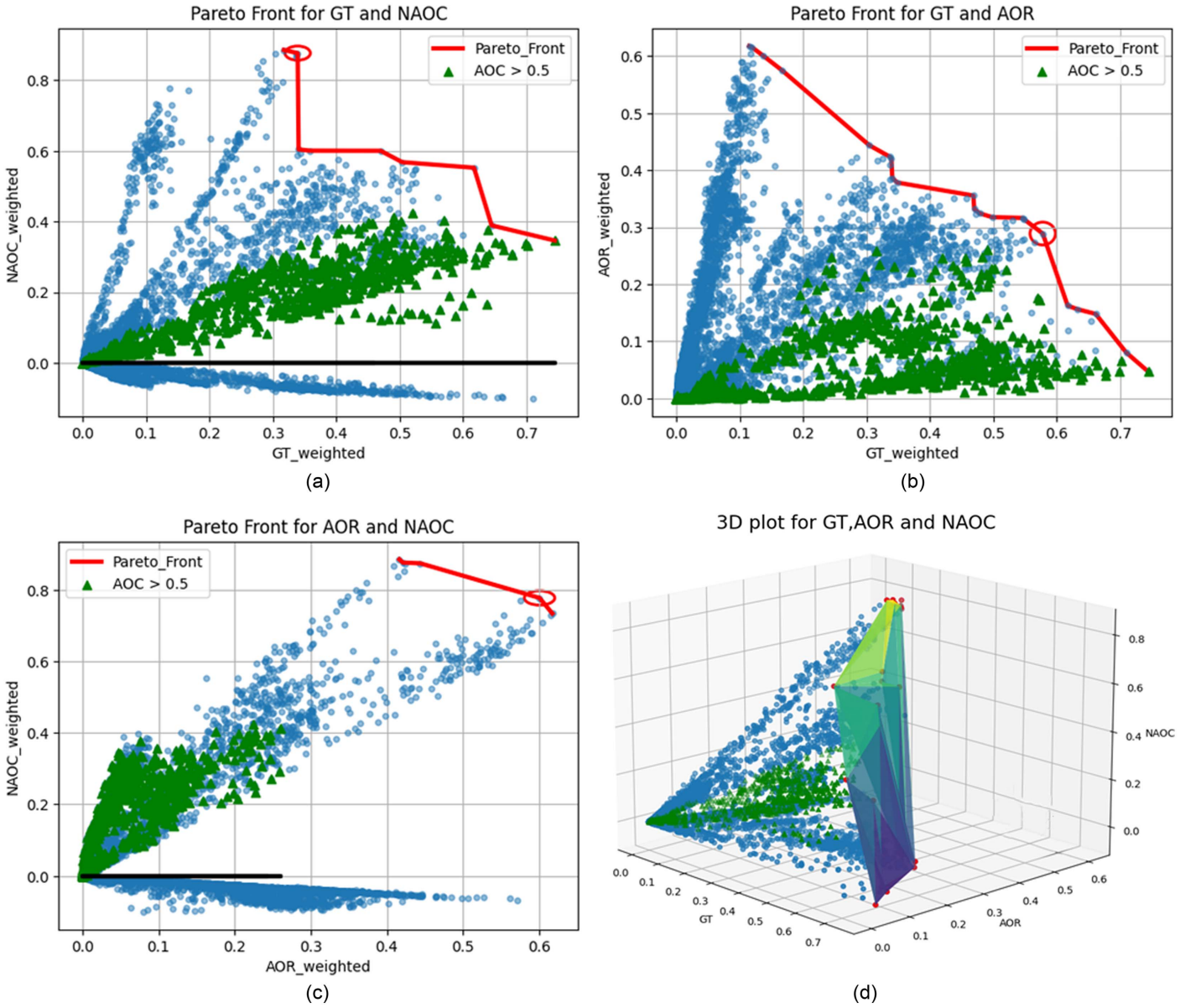

Fig. 4. Pareto front result for Case I: (a) GT and NAOC; (b) GT and AOR; (c) AOR and NAOC; and (d) 3D Pareto plane visualization.

Table 1. Final ranking results for Experiment I

INT	Phase	Time	Arrival	GT	AOR	AOC	Fig. ID	Rank
639	4	Nov Sat 1:00 PM–2:00 PM	883	**0.339**	0.421	**0.005**	4-a	1
639	4	Oct Sat 1:00 PM–2:00 PM	905	**0.318**	0.417	**0.018**	4-a	2
675	2	Nov Fri 6:00 PM–7:00 PM	940	**0.617**	0.162	**0.386**	4-a	3
670	2	Nov Tue 8:00 AM–9:00 AM	944	**0.578**	**0.289**	1.036	4-b	1
670	2	Nov Mon 7:00 AM–8:00 AM	936	**0.547**	**0.316**	1.027	4-b	2
670	2	Nov Mon 8:00 AM–9:00 AM	935	**0.548**	**0.314**	1.027	4-b	3
680	8	Nov Mon 3:00 PM–4:00 PM	783	0.137	**0.601**	**0.004**	4-c	1
680	8	Nov Mon 12:00 PM–1:00 PM	746	0.115	**0.618**	**0.010**	4-c	2
639	4	Nov Sat 3:00 PM–4:00 PM	878	0.304	**0.444**	**0.002**	4-c	3

Note: GT, AOR, and AOC shown are weighted numbers. Bold values indicate which two parameters are employed to compute the ranking score.

in the same top-right area. Table 2 presents the top three dominating approaches from each 2-D Pareto front, and three time-dependent bottlenecks were selected for verification:

1. Phase 2 at Intersection 675 from 6:00 PM to 7:00 PM on Friday in November 2021 with low AOC rates.
2. Phase 2 at Intersection 670 from 8:00 AM to 9:00 AM on Tuesdays in November 2021, experiencing excessive AOR.
3. Phase 8 at Intersection 680 from 11:00 AM to 12:00 AM on Monday in November 2021 has a high number of vehicles in red and arriving before or after the coordination.

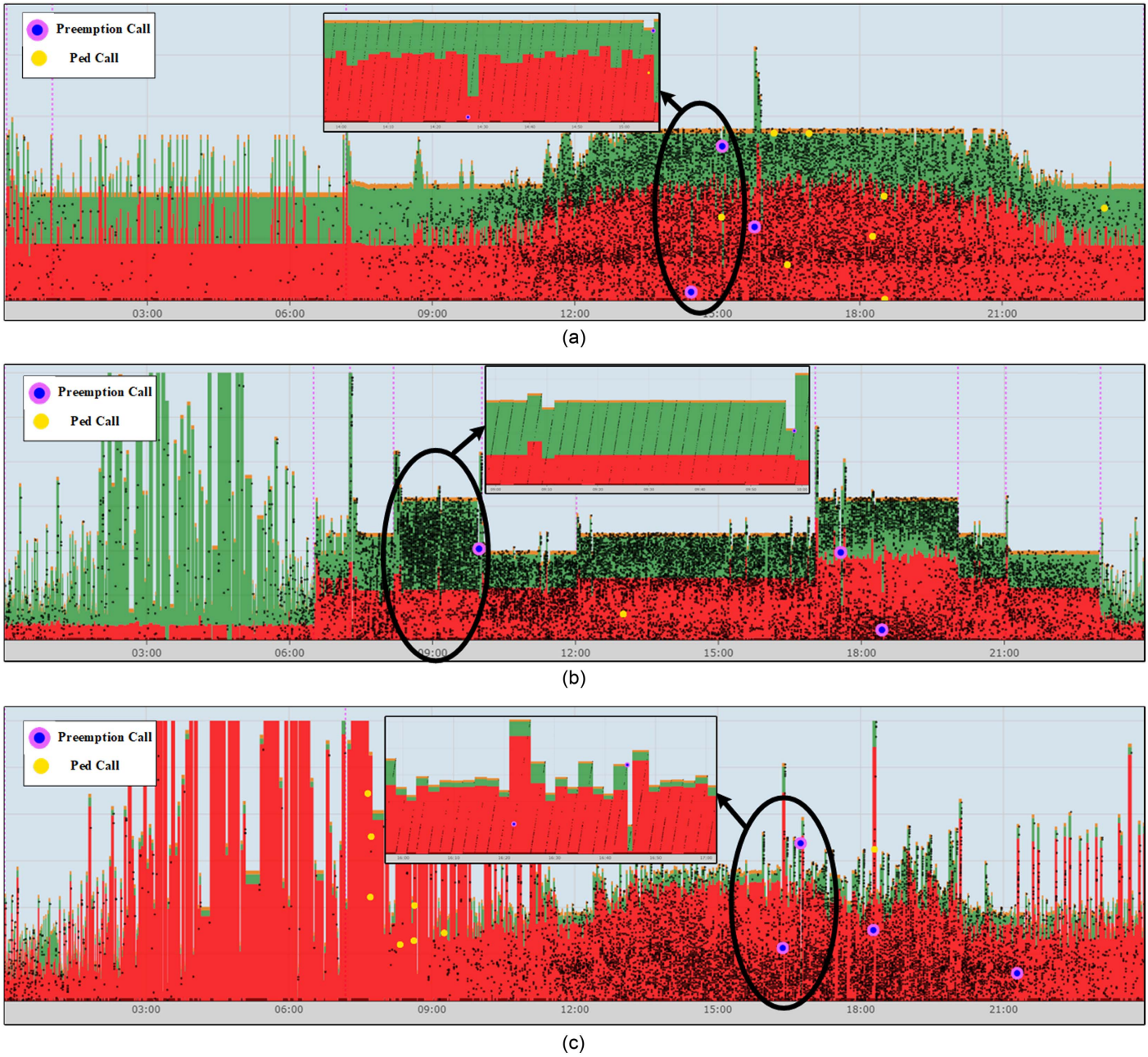

Fig. 5. PCDs for verifying dominating points in Case I: (a) GT versus AOC; (b) GT versus AOR; and (c) AOR versus AOC.

Three generated PCDs are displayed in Fig. 7 to help researchers identify the underlying problem at the bottleneck's periods.

Fig. 7(a) demonstrates a bottleneck during Phase 2 at Intersection 675 on Friday evening peak times. Based on PCD analysis, a preemption in Phase 4 was detected. This interruption affected the coordination and notably reduced the AOC. Fig. 7(b) illustrates that during Phase 2 at Intersection 670, there may be bottlenecks on Tuesdays in November 2021 between 8:00 AM and 9:00 AM. Despite adequate green time, many vehicles arrive during the red phase. PCD analysis confirms a significant number of vehicles arriving during this red phase in the morning peak, indicating a potential need to adjust the coordination plan. Meanwhile, Fig. 7(c) highlights Phase 8 of Intersection 680 on a Monday in November 2021, between 11:00 AM and 12:00 PM. Many vehicles arrive during the red phase, unable to align with the coordination plan. The PCD indicates that preemption and a shortened green time are likely causes, suggesting a reoptimization of the traffic signal timings is necessary.

Experiment III: Identifying Dominating Intersections Having Bottlenecks during Weekday Peak Hours

In this experiment, the focus remained on weekday peak hour data, while it was no longer concentrated on individual phases at a single intersection. Instead, the MOEs were calculated by averaging all phases together, allowing the mean MOE to represent the overall intersection signal performance during weekday peak hours. Data points were selected from weekdays (Monday to Friday) and within the AM peak hours (8 AM–10 AM), Midday peak hours (11 AM–1 PM) and PM peak hours (6 PM–8 PM). Fig. 8 presents three 2-D Pareto fronts with the top-ranked point circled in red, and Table 3 elaborates on three of the most dominant intersections from each

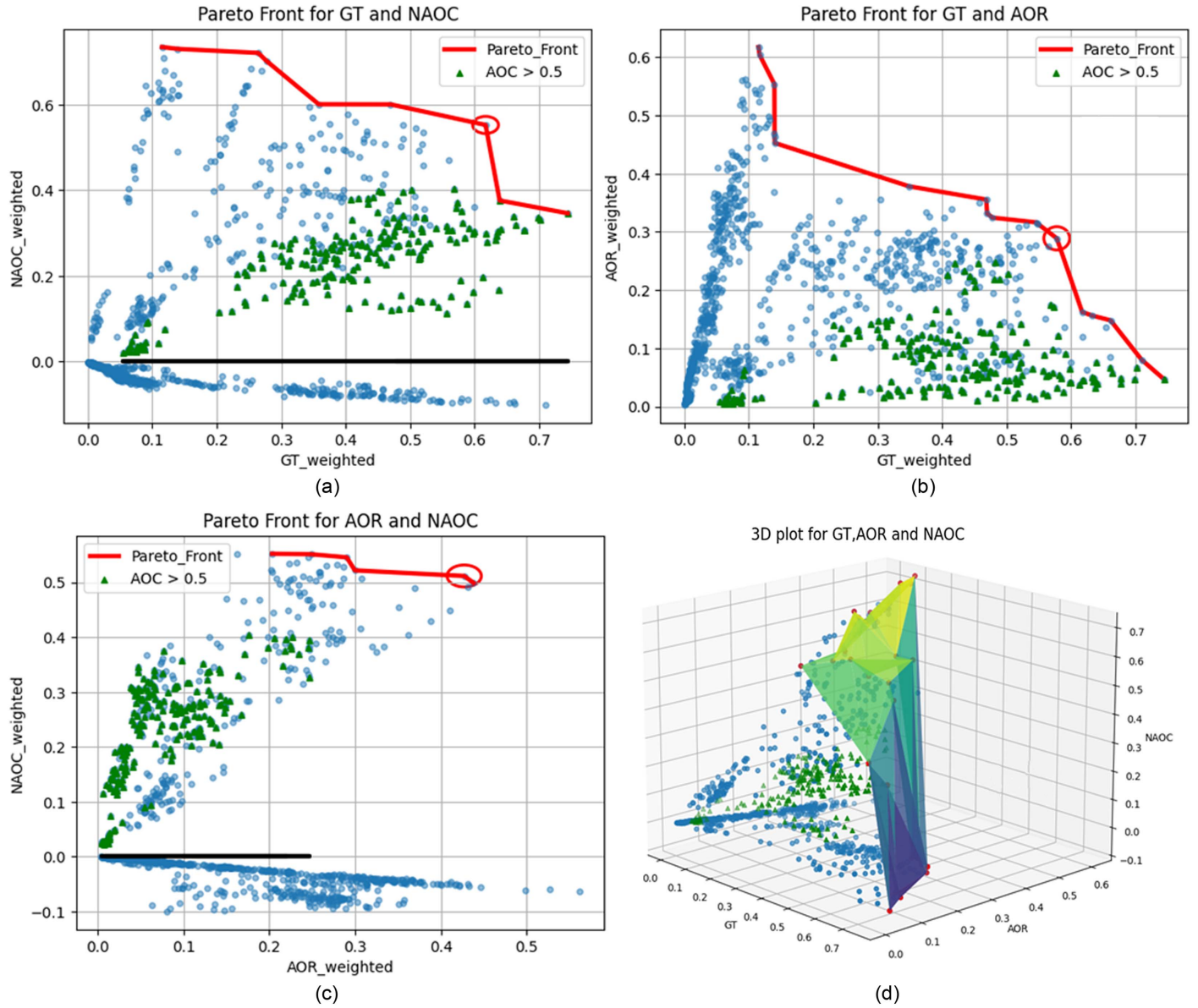

Fig. 6. Pareto front result for Case II: (a) GT and NAOC; (b) GT and AOR; (c)AOR and NAOC; and (d) 3D Pareto plane visualization.

Table 2. Final ranking results for Experiment II

INT	Phase	Time	Arrival	GT	AOR	AOC	Fig. ID	Rank
675	2	Nov Fri 6:00 PM–7:00 PM	940	**0.617**	0.162	**0.386**	6-a	1
673	6	Nov Fri 5:00 PM–6:00 PM	844	**0.744**	0.046	**0.497**	6-a	2
675	2	Nov Fri 11:00 AM–12:00 PM	891	**0.470**	0.332	**0.290**	6-a	3
670	2	Nov Tue 8:00 AM–9:00 AM	944	**0.578**	**0.289**	1.036	6-b	1
670	2	Nov Mon 7:00 AM–8:00 AM	936	**0.546**	**0.317**	1.027	6-b	2
670	2	Nov Mon 8:00 AM–9:00 AM	935	**0.548**	**0.314**	1.027	6-b	3
680	8	Nov Mon 11:00 AM–12:00 PM	519	0.084	**0.427**	**0.006**	6-c	1
680	8	Nov Wed 11:00 AM–12:00 PM	504	0.073	**0.438**	**0.003**	6-c	2
639	4	Oct Thu 6:00 PM–7:00 PM	593	0.223	**0.290**	**0.047**	6-c	3

Note: GT, AOR, and AOC shown are weighted numbers. Bold values indicate which two parameters are employed to compute the ranking score.

front. These three top-ranked scenarios from the Pareto front are then incorporated into the ATSPM to produce PCDs, as illustrated in Fig. 9.

Fig. 9(a) reveals a bottleneck at Intersection 639 on Fridays in November 2021, where numerous vehicles failed to capture the green band between 6:00 PM and 7:00 PM. Based on PCD, the researchers identified most vehicle arrivals during the red with a 37.3% AOC rate. Fig. 9(b) illustrates potential bottlenecks at Intersection 675 on Fridays in November 2021, occurring between 12:00 and 1:00 PM. A preemption event disrupted the existing

J. Transp. Eng., Part A: Systems, 2024, 150(5): 04024017

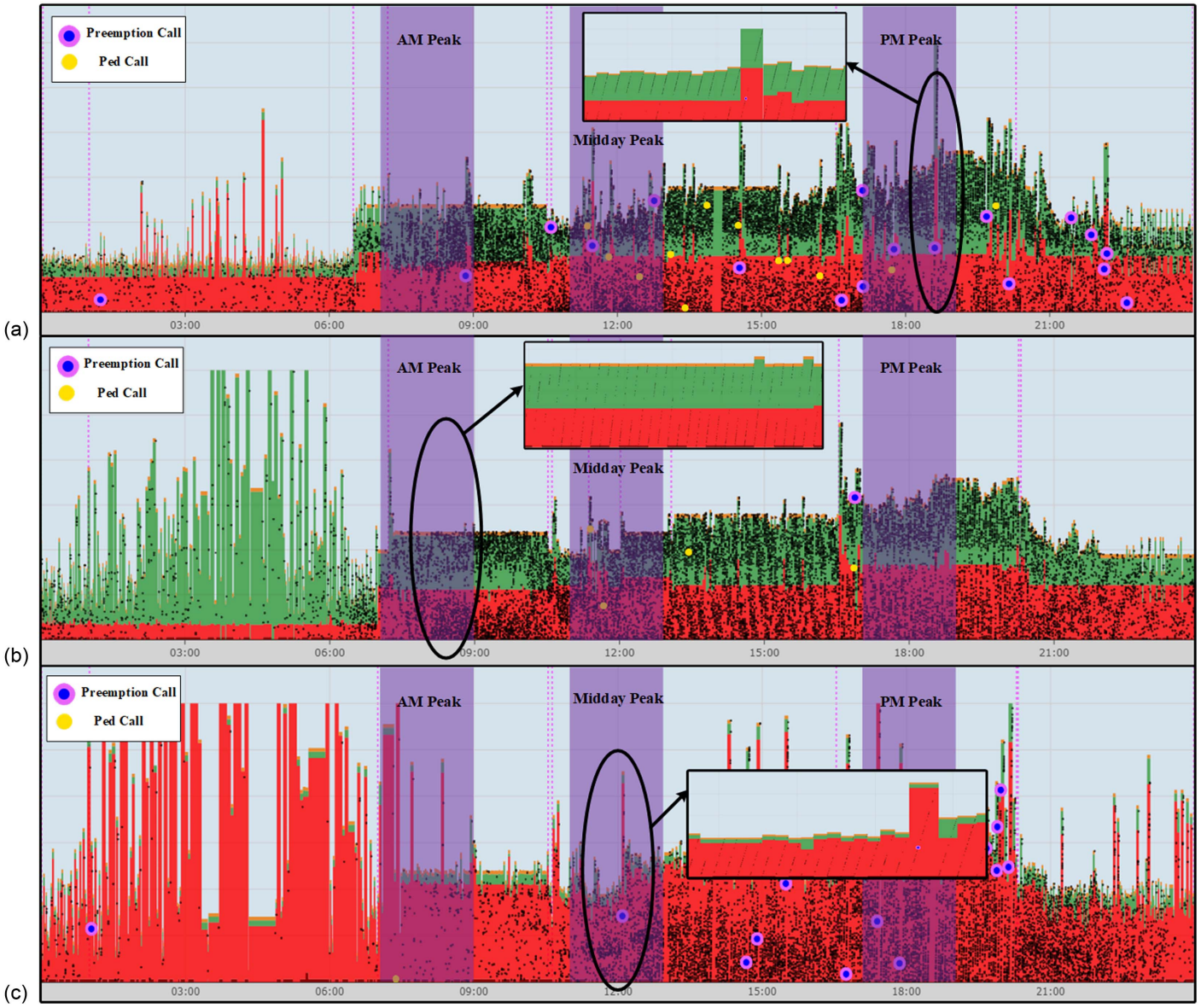

Fig. 7. PCDs for verifying dominating points in Case II: (a) GT versus AOC; (b) GT versus AOR; and (c) AOR versus AOC.

signal timing plan, causing an increasing percentage of vehicle arrivals during red. Fig. 9(c) highlights the concerns at Intersection 680 on a Friday in October 2021, specifically during the midday peak hours. Based on the PCD analysis, a significant number of vehicles arrive during red under the existing signal timing plan. Since Intersection 680 serves as a nexus between Preston Road and Stonebriar Centre, during the midday peak hour, the side street volume (547 vehicles per hour per lane) is nearly on par with the main street volume (704 vehicles per hour). It was believed that the current coordination plan overly prioritizes the main street. A more equitably balanced timing plan could mitigate this bottleneck.

Experiment IV: Cross Validate Ranking Results with Independent Connected Vehicle Data

To cross validate the proposed method, the connected vehicle data or the Wejo data set was adopted. The Wejo data represent a penetration rate of 2% to 6% of the overall vehicle population in the study area (Khadka et al. 2023). Typically, the CV data are abundant and encompasses a vast geographical area. Due to its high-resolution telematic nature, a few weeks of this CV dataset can amount to hundreds of gigabytes. Therefore, a systematic approach is crucial to effectively manage the data, ensure scalability, and eliminate outliers.

In this experiment, polygons were first generated on the global map system to represent the area of interest where the CV data were relevant to this problem, as depicted in Fig. 10. These polygons, established in the KML format, can be generated using geographic information system (GIS) software such as Google Earth or ArcGIS. Khadka et al. (2022) have introduced a scalable framework for processing data aimed at filtering out irrelevant details from the raw CV data, including waypoints that fall outside the intended scope. Readers are encouraged to refer to that source for a more comprehensive understanding of data reduction.

CV data contains a lot of vehicle dynamics information, including longitude, latitude, timestamp, and acceleration type. Among these parameters, the vehicle instantaneous speeds were commonly used to assess the level of intersection delay by calculating the

J. Transp. Eng., Part A: Systems, 2024, 150(5): 04024017

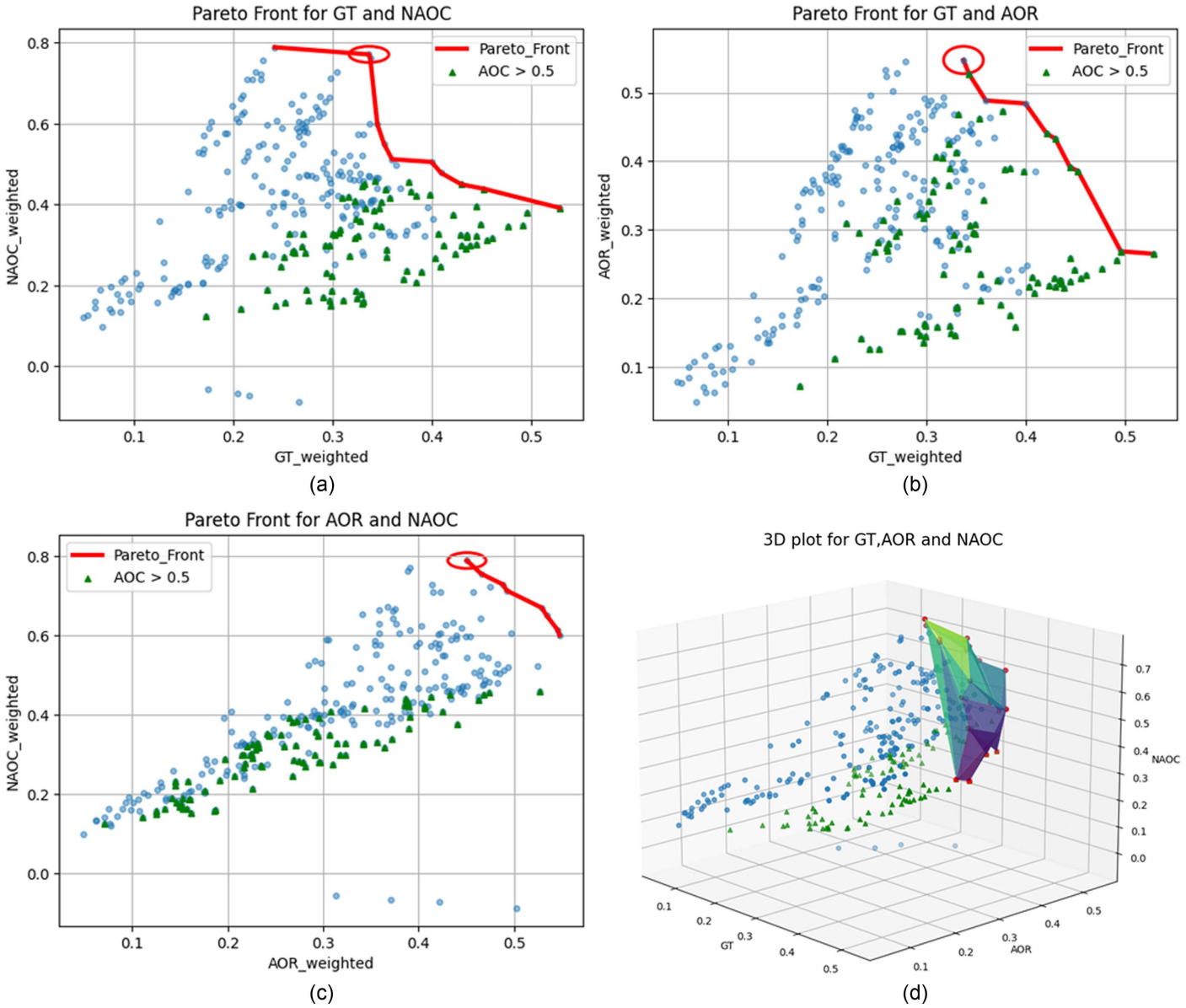

Fig. 8. Pareto front result for Case III: (a) GT and NAOC; (b) GT and AOR; (c) AOR and NAOC; and (d) 3D Pareto plane visualization.

Table 3. Final ranking results for Experiment III

INT	Time	Arrival	GT	AOR	AOC	Fig. ID	Rank
639	Nov Fri 5:00 PM–6:00 PM	530	**0.337**	0.390	**0.037**	8-a	1
639	Nov Fri 6:00 PM–7:00 PM	526	**0.338**	0.389	**0.039**	8-a	2
639	Nov Fri 12:00 PM–1:00 PM	520	0.242	0.451	0.004	8-a	3
675	Oct Fri 12:00 PM–1:00 PM	649	**0.337**	**0.548**	0.391	8-b	1
675	Nov Fri 6:00 PM–7:00 PM	656	**0.400**	**0.484**	0.495	8-b	2
675	Nov Mon 12:00 PM–1:00 PM	648	**0.343**	**0.527**	0.529	8-b	3
639	Oct Fri 12:00 PM–1:00 PM	520	0.242	**0.451**	**0.004**	8-c	1
639	Oct Mon 12:00 PM–1:00 PM	499	0.230	**0.466**	**0.006**	8-c	2
680	Nov Fri 5:00 PM–6:00 PM	593	0.305	**0.489**	**0.175**	8-c	3

Note: GT, AOR, and AOC shown are weighted numbers. Bold values indicate which two parameters are employed to compute the ranking score.

difference between actual travel time and free-flow travel time. Nonetheless, the vehicle speed samples varied significantly when making turns, and vehicles often moved faster than the speed limit. These identified features will make the delay estimation biased. Therefore, the researchers selected the precisely measured vehicles' control stops to indicate the mobility performance at intersections, and the control stops, excluding those instantaneous stop-and-goes, indicate heavy congestion.

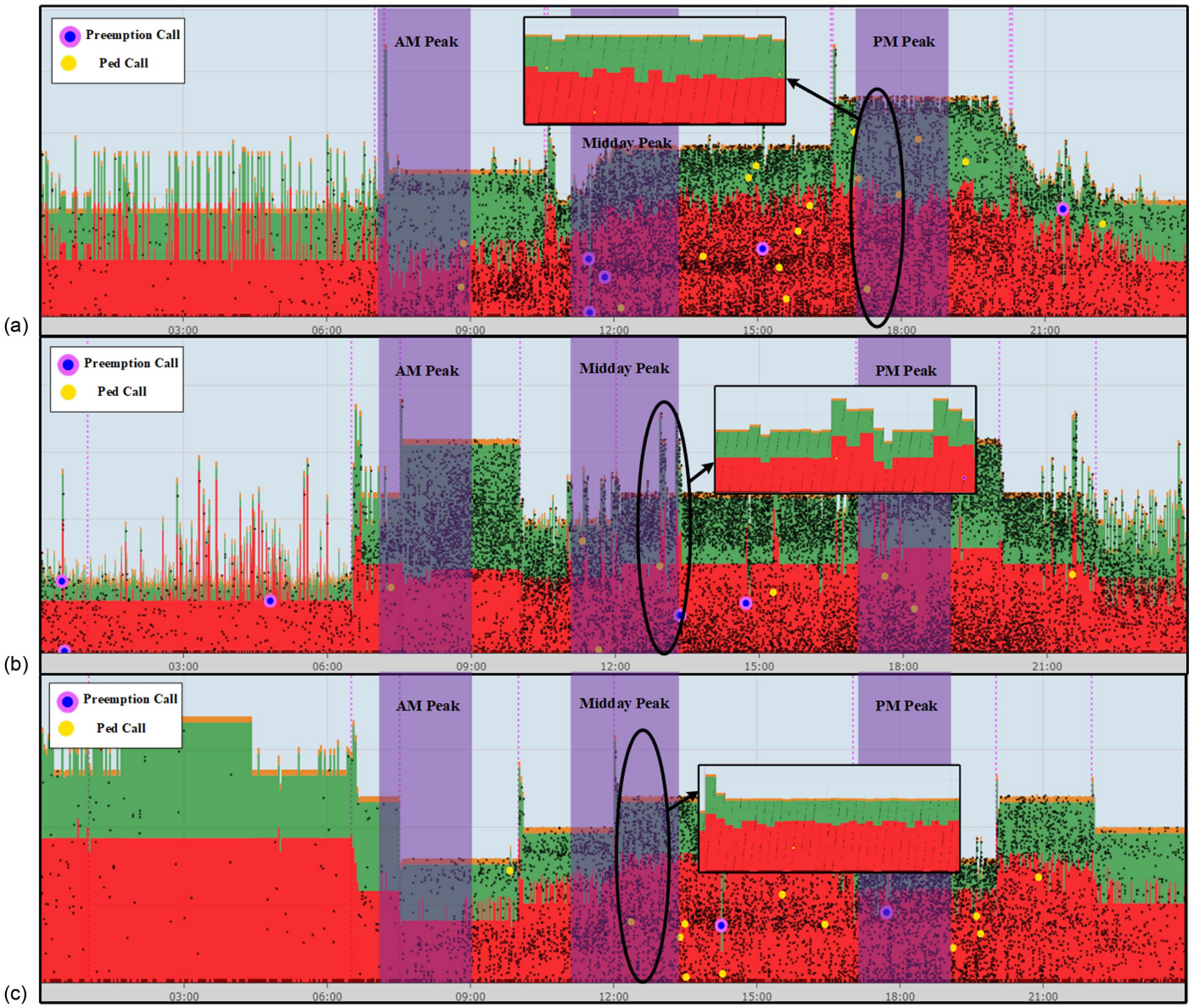

Fig. 9. PCDs for verifying dominating points in Case III: (a) GT versus AOC; (b) GT versus AOR; and (c) AOR versus AOC.

The control stops were extracted from the CV trajectory data, and the adopted threshold was that if a vehicle's instantaneous speed went slower than 5 mph or 7.33 fps, the subsequent waypoint speeds were checked. A control stop was identified if the slow status lasted longer than 6 s. The average was calculated after tallying all the control stops at an intersection. Lastly, all the approaches at each intersection are averaged, culminating in the overall average count of stops for each intersection. As an example, the time-of-day average vehicle control stops at Intersection 675 are shown in Fig. 11.

According to the plot, the midday peak recorded the highest average number of control stops, with the interval from 12 PM to 1 PM registering an average of 3.75 stops per vehicle to cross the intersection. In contrast, the morning peak hours seem to have good mobility, with only 1.16 control stops per vehicle. The evening peak witnessed 2.9 control stops per vehicle. The trend in the average number of stops correlates with the vehicle count trend shown in Fig. 3(a).

After the CV-data-based MOEs were developed, the researchers extracted the CV data covering the exact location and at the same time from the regional CV data set. The experiment was performed as follows:

1. Ranking the target intersections using multiple ATSPM MOEs and the Pareto front method presented in this paper to identify nine worst scenarios, three dominating points from each Pareto front, consisting of Experiments I, II, and III.
2. Processing the CV data calculating the average control stops for each scenario at the target intersection.
3. Using the Pareto front points as a reference, determine the average number of stops at the corresponding times and intersections indicated by these nine dominating points.

Two sets of intersection ranking, one based on the ATSPM MOEs and the other based on the CV data, are shown in Fig. 12, and more details are in Table 4. In Fig. 12, the average stops per hour for each workday at the five intersections are represented by blue dots (taking blue points on Monday in Fig. 12 as an example, the blue dots represent the hourly average number of stops from all five intersections). The color areas—red, orange, and yellow—denote the top 10%, 20%, and 30% worst scenarios based on the

J. Transp. Eng., Part A: Systems, 2024, 150(5): 04024017

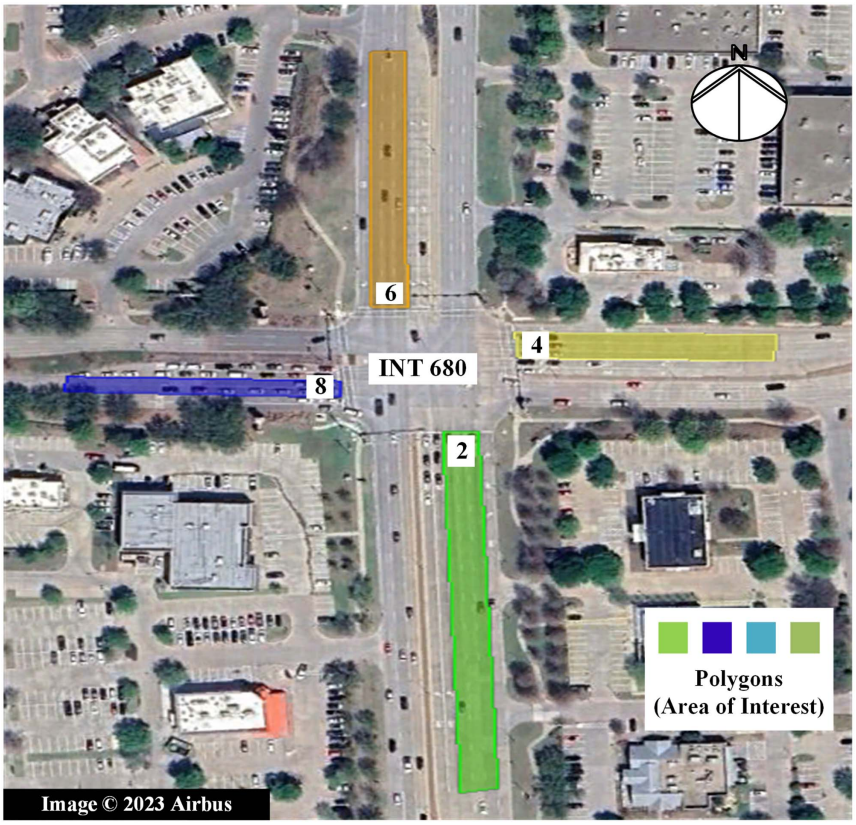

Fig. 10. Generating polygons for an area of interest. (Image ©2023 Airbus.)

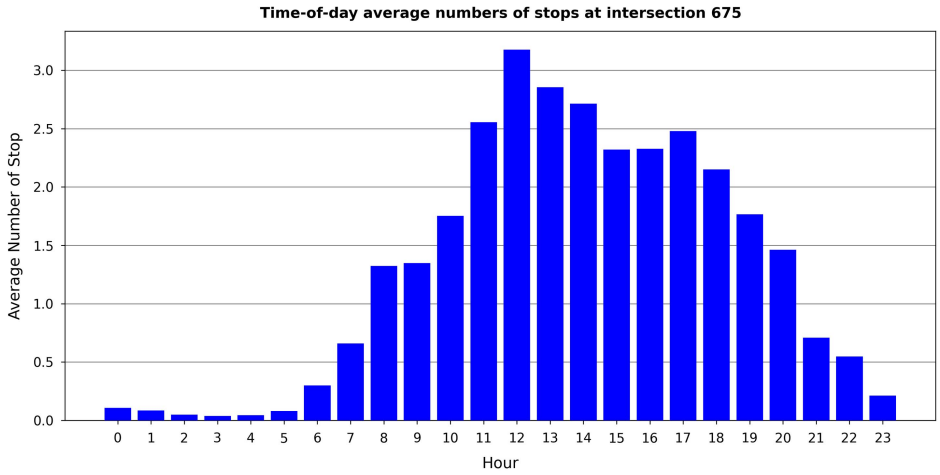

Fig. 11. Time-of-day average number of stops plot.

average number of stops calculated from the CAV dataset. Subsequently, the identified Pareto front points (PFP) derived from the proposed method are marked as red diamonds on the same plot, aligned with the corresponding times. Even though the intersection rankings based on two data sets (ATSPM data versus CV data) do not (and should not) match exactly, it is apparent that the two intersection rankings reveal consistency.

From Fig. 12 and Table 4, the following remarks can be made:

1. Most of the identified worst scenarios fell into the top 30% of worst scenarios in which the CV data reported the highest control stops per vehicle.
2. One worst scenario out of the Pareto front in each experiment does not fall within the top 30% of worst scenarios in which the CV data reported the highest control stops per vehicle.

The two ranking methods and data sources are heterogeneous in nature, and they are expected not to match exactly. While the CV data were primarily collected with high fidelity, the inherent positioning error in the CV data may influence the result. Also, the lane-width polygon may retrieve irrelevant CV data samples out of the polygons. On the other hand, the ATSPM data collection in practice faces many challenges such as clock synchronization among intersections, detector accuracy, and reliability. These challenges may

J. Transp. Eng., Part A: Systems, 2024, 150(5): 04024017

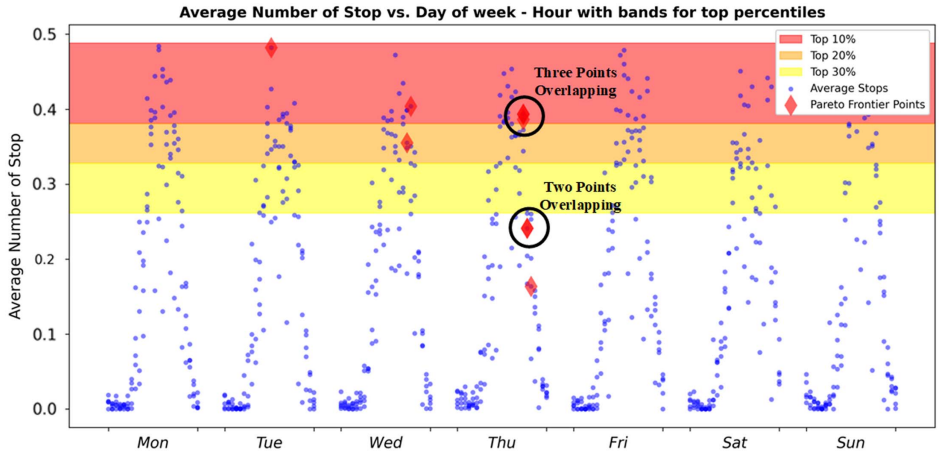

Fig. 12. Average number of stops based on day-of-week–hour plot.

Table 4. Final ranking results for Experiment IV

INT	Time	Number of stops	Average number of stops	Pareto front name	Rank by PFP	Rank by Wejo	Top (%)
675	Thu 5:00 PM–6:00 PM	14.250	**0.393**	AOR NAOC	1	1	10
675	Thu 6:00 PM–7:00 PM	10.063	**0.241**	AOR NAOC	2	3	—
639	Thu 5:00 PM–6:00 PM	6.938	**0.386**	AOR NAOC	3	2	10
675	Thu 7:00 PM–8:00 PM	7.313	**0.164**	GT AOR	1	3	—
675	Wed 5:00 PM–6:00 PM	13.313	**0.356**	GT AOR	2	2	20
675	Tue 12:00 PM–1:00 PM	17.625	**0.482**	GT AOR	3	1	10
675	Thu 5:00 PM–6:00 PM	14.250	**0.393**	GT NAOC	1	2	10
675	Thu 6:00 PM–7:00 PM	10.063	**0.241**	GT NAOC	2	3	—
639	Wed 6:00 PM–7:00 PM	6.750	**0.404**	GT NAOC	3	1	10

Note: Bold values indicate which two parameters are employed to compute the ranking score.

also bring additional bias to the proposed framework. Nonetheless, the ATSPM data quality and its impact on the proposed intersection ranking framework is out of the scope of this paper. Despite these differences and challenges, the two ranking methods indeed reveal the same consistency.

Discussion

Three experiments reflecting agencies' needs were conducted, and one more experiment was conducted to cross validate results based on an independent data source, the CV data set. Experiments I and II aim to help agencies understand the spatiotemporal characteristics of intersection bottlenecks based on the ATSPM MOEs under different scenarios. The outcome provides decision support on signal timing improving gradually. Experiment III aims to help agencies identify problematic intersections to prioritize their regional intersection improvement plan. Experiment IV validated the proposed method by cross validating the ranking results with another ranking method based on the CV data set. Both methods and data sets are being used in practice, and they showed acceptable consistency in this experiment.

Conclusions and Future Work

In this paper, we explored using the automatically generated ATSPM MOEs and multiobjective Pareto front method to rank the time-dependent performance of target intersections and identify the spatiotemporal characteristics of bottlenecks. The objective is to facilitate agencies to identify problematic intersections and reduce their efforts in visualizing the ATSPM MOEs. In congested urban areas, bottlenecks at intersections often appear, disappear, and reappear multiple times daily. The emerging ATSPM system is adequate to identify these bottlenecks and their causes. Nonetheless, after more and more intersections can generate the ATSPM data, aggregating and visualizing the ATSPM MOEs at all intersections is overwhelming agencies to exploit the benefits of ATSPM systems further. To address this issue, we develop an automated framework to identify the most problematic approaches at intersections based on the ATSPM MOEs. An add-on module was developed to continuously generate the ATSPM MOEs rather than generate them upon user's requests. Four experiments were conducted in the case study, including five intersections on Preston Road in Frisco, Texas, to find the worst scenarios and possible mitigations. The results were compared with the congestion ranking based on the CV data and showed acceptable consistency.

In the future, we plan to (1) add new features to mitigate the ATSPM data quality issue like missing and biased estimation; (2) develop scalable computing methods to identify problematic intersections among hundreds or thousands of intersections. The overarching goal is to evolve the ATSPM system to better inform and support decisions on arterial traffic management.

Data Availability Statement

Some or all data, models, or codes that support the findings of this study are available from the corresponding author upon reasonable request.

Acknowledgments

The authors thank the City of Frisco in Texas for offering access to their traffic control network and ATSPM database. Any opinions, findings, conclusions, or recommendations expressed in this paper are solely those of the authors. They do not necessarily reflect the official views or policies of the above organizations, nor do the contents constitute a standard, specification, or regulation of these organizations. The CV data were distributed by Wejo Data Service Inc.

References

Abbas, M. M., and A. Sharma. 2006. "Multiobjective plan selection optimization for traffic responsive control." *J. Transp. Eng.* 132 (5): 376–384. https://doi.org/10.1061/(ASCE)0733-947X(2006)132:5(376).

Abbott-Jard, M., H. Shah, and A. Bhaskar. 2013. "Empirical evaluation of Bluetooth and Wifi scanning for road transport." In *Proc., 36th Australasian Transport Research Forum (ATRF)*. West Lafayette, IN: Purdue Univ.

Arrow, K. J., and G. Debreu. 1954. "Existence of an equilibrium for a competitive economy." *Econometrica* 22 (3): 265–290. https://doi.org/10.2307/1907353.

Balke, K. N., H. A. Charara, and R. Parker. 2005. *Development of a traffic signal performance measurement system (TSPMS)*. College Station, TX: Texas Transportation Institute, Texas A & M Univ. System College.

Balke, K. N., and C. Herrick. 2004. *Potential measures of assessing signal timing performance using existing technologies*. Austin, TX: Texas Transportation Institute, Texas A & M Univ. System College.

Barcelö, J., L. Montero, L. Marqués, and C. Carmona. 2010. "Travel time forecasting and dynamic origin-destination estimation for freeways based on Bluetooth traffic monitoring." *Transp. Res. Rec.* 2175 (1): 19–27. https://doi.org/10.3141/2175-03.

Brennan, T. M., Jr., C. M. Day, J. R. Sturdevant, and D. M. Bullock. 2011. "Visual education tools to illustrate coordinated system operation." *Transp. Res. Rec.* 2259 (1): 59–72. https://doi.org/10.3141/2259-06.

Chellapilla, H., R. Sivanandan, B. R. Chilukuri, and C. Rajendran. 2023. "Bi-objective optimization models for mitigating traffic congestion in urban road networks." *J. Traffic Transp. Eng. (English Ed.)* 10 (1): 86–103. https://doi.org/10.1016/j.jtte.2021.09.006.

David Schrank, L. A., Bill Eisele, and Tim Lomax. 2021. *2021 Urban mobility report*. College Station, TX: Texas A&M Transportation Institute.

Day, C. M., D. M. Bullock, H. Li, S. M. Lavrenz, W. B. Smith, and J. R. Sturdevant. 2016. *Integrating traffic signal performance measures into agency business processes*. West Lafayette, IN: Purdue Univ.

Day, C. M., D. M. Bullock, H. Li, S. M. Remias, A. M. Hainen, R. S. Freije, A. L. Stevens, J. R. Sturdevant, and T. M. Brennan. 2014. *Performance measures for traffic signal systems: An outcome-oriented approach*. West Lafayette, IN: Purdue Univ.

Day, C. M., E. J. Smaglik, D. M. Bullock, and J. R. Sturdevant. 2008. *Real-time arterial traffic signal performance measures*. West Lafayette, IN: Purdue Univ.

Grossman, J., and D. M. Bullock. 2013. *Performance measures for local agency traffic signals*. West Lafayette, IN: Purdue Univ.

Jiao, P., R. Li, and Z. Li. 2016. "Pareto front–based multi-objective real-time traffic signal control model for intersections using particle swarm optimization algorithm." *Adv. Mech. Eng.* 8 (8): 168781401666604. https://doi.org/10.1177/1687814016666042.

Jin, P. J., T. Zhang, T. M. Brennan Jr., and M. Jalayer. 2019. *Real-time signal performance measurement (RT-SPM)*. Washington, DC: DOT, Federal Highway Administration.

Khadka, S., P. T. Li, and Q. Wang. 2022. "Developing novel performance measures for traffic congestion management and operational planning based on connected vehicle data." *J. Urban Plann. Dev.* 148 (2): 04022016. https://doi.org/10.1061/(ASCE)UP.1943-5444.0000835.

Khadka, S., P. S. Wang, P. T. Li, and F. J. Torres. 2023. "A new framework for regional traffic volumes estimation with large-scale connected vehicle data and deep learning method." *J. Transp. Eng. Part A. Syst.* 149 (4): 04023015. https://doi.org/10.1061/JTEPBS.TEENG-7536.

Li, P., F. R. Chowdhury, P. Wang, and S. M. Imtiaz. 2020. "Actuated traffic signal performance evaluation along arterials using wi-fi travel time samples and high-resolution traffic signal events data." *Transp. Res. Rec.* 2674 (6): 268–280. https://doi.org/10.1177/0361198120918869.

Liu, H. X., and W. Ma. 2009. "A virtual vehicle probe model for time-dependent travel time estimation on signalized arterials." *Transp. Res. Part C Emerging Technol.* 17 (1): 11–26. https://doi.org/10.1016/j.trc.2008.05.002.

Ngatchou, P., A. Zarei, and A. El-Sharkawi. 2005. "Pareto multi objective optimization." In *Proc., 13th Int. Conf. on, Intelligent Systems Application to Power Systems*, 84–91. New York: IEEE.

Pishue, B. 2021. *2021 INRIX global traffic scorecard*. Kirkland, WA: INRIX.

Pitton, A.-C., A. Vassilev, and S. Charbonnier. 2012. "Vehicle re-identification with several magnetic sensors." In *Proc., Advanced Microsystems for Automotive Applications 2012: Smart Systems for Safe, Sustainable and Networked Vehicles*, 281–290. Berlin: Springer.

Q-Free. 2023. "Intelight-MaxView." Accessed January 9, 2023. https://www.q-free.com/product/intelight-maxview/.

Remias, S. M., J. Waddell, M. Klawon, and K. Yang. 2018. *Signal performance measures pilot implementation*. Lansing, MI: Michigan DOT, Research Administration.

Sharma, A., D. M. Bullock, and J. A. Bonneson. 2007. "Input–output and hybrid techniques for real-time prediction of delay and maximum queue length at signalized intersections." *Transp. Res. Rec.* 2035 (1): 69–80. https://doi.org/10.3141/2035-08.

Smaglik, E. J., A. Sharma, D. M. Bullock, J. R. Sturdevant, and G. Duncan. 2007. "Event-based data collection for generating actuated controller performance measures." *Transp. Res. Rec.* 2035 (1): 97–106. https://doi.org/10.3141/2035-11.

Sturdevant, J. R., T. Overman, E. Raamot, R. Deer, D. Miller, D. M. Bullock, C. M. Day, T. M. Brennan Jr., H. Li, and A. Hainen. 2012. *Indiana traffic signal hi resolution data logger enumerations*. West Lafayette, IN: Purdue Univ.

TransIntelligence. 2023. "Transync suite signal timing diagnosis & optimization." Accessed September 26, 2023. http://trans-intelligence.com/index.html.

US DOT. 2018. *Automated traffic signal performance measures case studies. Utah Department of Transportation*. Washington, DC: US DOT.

Zhao, J., J. Yu, and X. Zhou. 2019. "Saturation flow models of exit lanes for left-turn intersections." *J. Transp. Eng. Part A. Syst.* 145 (3): 04018090. https://doi.org/10.1061/JTEPBS.0000204.